

# Spin glass model of in-context learning

Yuhao Li<sup>1</sup>, Ruoran Bai<sup>1</sup>, and Haiping Huang<sup>1,2\*</sup>

<sup>1</sup>*PMI Lab, School of Physics, Sun Yat-sen University,  
Guangzhou 510275, People's Republic of China and*

<sup>2</sup>*Guangdong Provincial Key Laboratory of Magnetoelectric Physics and Devices,  
Sun Yat-sen University, Guangzhou 510275, People's Republic of China*

(Dated: November 14, 2024)

Large language models show a surprising in-context learning ability—being able to use a prompt to form a prediction for a query, yet without additional training, in stark contrast to old-fashioned supervised learning. Providing a mechanistic interpretation and linking the empirical phenomenon to physics are thus challenging and remain unsolved. We study a simple yet expressive transformer with linear attention and map this structure to a spin glass model with real-valued spins, where the couplings and fields explain the intrinsic disorder in data. The spin glass model explains how the weight parameters interact with each other during pre-training, and further clarifies why an unseen function can be predicted by providing only a prompt yet without further training. Our theory reveals that for single-instance learning, increasing the task diversity leads to the emergence of in-context learning, by allowing the Boltzmann distribution to converge to a unique correct solution of weight parameters. Therefore the pre-trained transformer displays a prediction power in a novel prompt setting. The proposed analytically tractable model thus offers a promising avenue for thinking about how to interpret many intriguing but puzzling properties of large language models.

*Introduction.*— Thanks to earlier breakthroughs in processing natural languages (e.g., translation), vector representation and attention concepts were introduced into machine learning [1–4], which further inspired a recent breakthrough of implementing the self-attention as a feedforward model of information flow, namely transformer [5]. The self-attention captures dependencies between different parts of the input (e.g., image or text), coupled with a simple cost of next-token prediction [6, 7], leading to a revolution in the field of natural language processing [8], so-called large language model (LLM).

One of the astonishing abilities of the transformer is the in-context learning [9], i.e., the pre-trained transformer is able to accomplish previously-unseen complicated tasks by showing a short prompt in the form of instructions and a handful of demonstrations, especially without a need for updating the model parameters. LLMs thus develop a wide range of abilities and skills (e.g., question answering, code generation) [10], which are not explicitly contained in the training dataset and are not specially designed to optimize. This remarkable property is achieved only by training for forecasting the next tokens and only if corpus and model sizes are scaled up to a huge number [11, 12]. The above characteristics of transformer and the in-context learning (ICL) are in stark contrast to perceptron models in the standard supervised learning context, presenting a formidable challenge for a mechanistic interpretation [13, 14].

To achieve a scientific theory of ICL, previous works focused on optimization via gradient descent dynamics [15, 16], representation capacity [17], Bayesian inference [18, 19], and in particular the pre-training task diversity [19–22]. The theoretical efforts were commonly based on a single-layer linear attention [15, 21, 23, 24], which revealed that a sufficient pre-training task diver-

sity guarantees the emergence of ICL, i.e., the model can generalize beyond the scope of pre-training tasks.

However, rare connections are established to physics models, which makes a physics model of ICL lacking so far, preventing us from a deep understanding of how ICL emerges from pre-trained model parameters. Here, we treat the transformer learning as a statistical inference problem, and then rephrase the inference problem as a spin glass model, where the transformer parameters are turned into real-valued spins, and the input sequences act as a quenched disorder, which makes the spins strongly interact with each other to lower down the ICL error. A unique spin solution exists in the model, guaranteeing that the transformer can predict the unknown function embedded in test prompts. The derived formulas specify the intelligence boundary of ICL and how this can be achieved.

*Transformer with linear attention.*— We consider a simple transformer structure—a single-layer self-attention transforming an input sequence to an output one. Given an input sequence  $\mathbf{X} \in \mathbb{R}^{D \times N}$ , where  $D$  is the embedding dimension and  $N$  is the context length, the self-attention matrix is a softmax function  $\text{Softmax}(\mathbf{Q}^\top \mathbf{K} / \sqrt{D})$ , where  $\mathbf{Q} = \mathbf{W}_Q \mathbf{X}$ ,  $\mathbf{K} = \mathbf{W}_K \mathbf{X}$ .  $\mathbf{W}_Q$  and  $\mathbf{W}_K$  are the query and key matrices ( $\in \mathbb{R}^{D \times D}$ ), respectively.  $\sqrt{D}$  inside the softmax function makes its argument order of unity. The self-attention refers to the attention matrix generated from the input sequence itself and allows each element (query) to attend to all other elements in one input sequence, being learnable through pre-training. The softmax function is thus calculated independently for each row. Taking an additional transformation  $\mathbf{V} = \mathbf{W}_V \mathbf{X}$ , where  $\mathbf{W}_V \in \mathbb{R}^{D \times D}$  is the value matrix, one can generate the output  $\mathbf{Y} = \mathbf{V} \cdot \text{Softmax}(\mathbf{Q}^\top \mathbf{K} / \sqrt{D})$ . Hence, this simple transformer

implements a function  $\varphi_{\text{TF}}(\mathbf{X}) : \mathbb{R}^{D \times N} \rightarrow \mathbb{R}^{D \times N}$ .

For simplicity, we replace the computationally expensive softmax by linear attention, which is *still expressive* [25]. Defining  $\mathbf{W} \equiv \mathbf{W}_Q^\top \mathbf{W}_K$ , and choosing  $\mathbf{W}_V = \mathbf{1}_D$  ( $\mathbf{1}_D$  indicates a  $D \times D$  identity matrix) for our focus on the query and key matrices, we re-express the linear transformer as  $\mathbf{Y} = \frac{1}{DN} \mathbf{X} \mathbf{X}^\top \mathbf{W} \mathbf{X}$ , where  $\mathbf{X}$  contains prompts and the query (to be predicted by the transformer), and  $\mathbf{W} \in \mathbb{R}^{D \times D}$  is the equivalent weight matrix to be trained, and  $\frac{1}{DN}$  is a normalization coefficient.

We next design the training task as a high-dimensional linear regression. Each example consists of the data  $\mathbf{x} \sim \mathcal{N}(0, \mathbf{1}_D)$  and the corresponding label  $y = \mathbf{w}^\top \mathbf{x}$ , where the latent task weight  $\mathbf{w} \sim \mathcal{N}(0, \mathbf{1}_D)$ . To construct the  $\mu$ -th input matrix  $\mathbf{X}^\mu$ , we use  $N$  samples as prompts using the same  $\mathbf{w}^\mu$  yet different  $\mathbf{x}$  within the input sequence. An additional sample  $\tilde{\mathbf{x}}^\mu$  is regarded as the query whose true label  $\tilde{y}$  is masked yet to be predicted by the transformer. The structure of each input matrix  $\mathbf{X}^\mu$  is thus represented as

$$\mathbf{X}^\mu = \begin{bmatrix} \mathbf{x}_1^\mu & \mathbf{x}_2^\mu & \cdots & \mathbf{x}_n^\mu & \tilde{\mathbf{x}}^\mu \\ y_1^\mu & y_2^\mu & \cdots & y_n^\mu & 0 \end{bmatrix} \in \mathbb{R}^{(D+1) \times (N+1)}. \quad (1)$$

Due to this form of the input matrix, the number of trainable elements in  $\mathbf{W}$  becomes  $(D+1)^2$ . The last element of  $\mathbf{Y}$  corresponds to the predicted label of the query  $\tilde{\mathbf{x}}^\mu$ , i.e.,  $\hat{y}^\mu = \mathbf{Y}_{D+1, N+1}^\mu$ . The goal of ICL is to use the prompt to form a prediction for the query, and the true function governing the linear relationship for the testing prompt is hidden during pre-training, because each  $\mu$  is generated by an independently drawn  $\mathbf{w}$  during both training and test phases. We consider an ensemble of  $P$  sequences, and  $P$  is thus called the task diversity. This setting is a bit different from that in recent works [19, 21].

The pre-training is carried out by minimizing the mean squared error function, and the total training loss is given by

$$\mathcal{L} = \frac{1}{2P} \sum_{\mu} (\tilde{y}^\mu - \hat{y}^\mu)^2 + \frac{\lambda}{2} \|\mathbf{W}\|^2, \quad (2)$$

where  $\lambda$  controls the weight-decay strength. The generalization error on unseen tasks is written as  $\epsilon_g = \mathbb{E}_{\tilde{\mathbf{x}}, \mathbf{x}, \mathbf{w}} (\tilde{y} - \hat{y})^2$ , where the ensemble average over all disorders is considered.

*Spin-glass model mapping.*— Equation (2) can be treated as a Hamiltonian in statistical physics. The linear attention structure makes the spin-model mapping possible. This proceeds as follows. The prediction to the  $\mu$ -th input matrix can be recast as  $\hat{y}^\mu = (DN)^{-1} \sum_{m,n} \mathbf{C}_{D+1,m}^\mu \mathbf{W}_{m,n} \mathbf{X}_{n,N+1}^\mu$ , where  $\mathbf{C}^\mu \equiv \mathbf{X}^\mu \mathbf{X}^{\mu \top}$ . Then we define an index mapping  $\Gamma : (m, n) \rightarrow i$  to flatten a matrix into a vector. Therefore, one can write  $\sigma_i = \Gamma \mathbf{W}_{m,n}$ , and  $s_i^\mu = (DN)^{-1} \Gamma \mathbf{C}_{D+1,m}^\mu \mathbf{X}_{n,N+1}^\mu$ , where  $i = (D+1)(m-1) + n$ , and finally the prediction

as  $\hat{y}^\mu = \sum_i s_i^\mu \sigma_i$ . Consequently, the mean-squared error for each input matrix reads

$$\ell^\mu = \frac{1}{2} \sum_{i,j} s_i^\mu s_j^\mu \sigma_i \sigma_j - \tilde{y}^\mu \sum_i s_i^\mu \sigma_i, \quad (3)$$

where we omit the constant term  $(\tilde{y}^\mu)^2/2$ .

Upon defining  $J_{ij}^\mu \equiv -s_i^\mu s_j^\mu$ ,  $h_i^\mu \equiv \tilde{y}^\mu s_i^\mu$ , and  $\lambda_i^\mu \equiv \lambda - J_{ii}^\mu$ , one can rewrite the total loss  $\mathcal{L} = (1/P) \sum_{\mu} \ell^\mu + \frac{1}{2} \lambda \|\mathbf{W}\|^2$  as

$$\mathcal{L} = -\frac{1}{2P} \sum_{\mu, i, j} J_{ij}^\mu \sigma_i \sigma_j - \frac{1}{P} \sum_{\mu, i} h_i^\mu \sigma_i + \frac{1}{2} \lambda \sum_i \sigma_i^2. \quad (4)$$

By moving the elements for  $i = j$  in the first term to the regularization term, and defining an anisotropic regularization coefficient  $\lambda_i^\mu \equiv \lambda - J_{ii}^\mu$ , we can formally define the effective interaction  $J_{ij} \equiv (1/P) \sum_{\mu} J_{ij}^\mu$ , the external field  $h_i \equiv (1/P) \sum_{\mu} h_i^\mu$  and the regularization factor  $\lambda_i \equiv (1/P) \sum_{\mu} \lambda_i^\mu$ . Finally, we obtain a spin glass model with the following Hamiltonian

$$\mathcal{H}(\boldsymbol{\sigma}) = -\sum_{i < j} J_{ij} \sigma_i \sigma_j - \sum_i h_i \sigma_i + \frac{1}{2} \sum_i \lambda_i \sigma_i^2, \quad (5)$$

where the total number of spins is given by  $(D+1)^2$ .

The disorder in the pre-training dataset including the diversity in the latent task vectors  $\mathbf{w}$  is now encoded into the interactions between spins, and random fields the spins feel. In fact, this is a densely connected spin glass model, while the coupling and field statistics do not have an analytic expression [26], as they bear a fat tail (Fig. 1). This reminds us of the two-body spherical spin model studied in spin glass theory [27, 28], but the current glass model of ICL seems much more complex than the spherical model. By construction, this model reflects the nature of associative memory [29], yet the spin variable is now the underlying parameter of the transformer. To conclude, we derive a spin glass model of ICL, opening a physically appealing route towards the mechanistic interpretation of ICL and even more complex transformers (see extra experiments in [30]).

*Statistical mechanics analysis.*— The probability of each weight configuration is given by the Gibbs-Boltzmann distribution  $P(\boldsymbol{\sigma}) = e^{-\beta \mathcal{H}(\boldsymbol{\sigma})} / Z$ , where  $Z$  is the partition function, and  $\beta$  is an inverse temperature tuning the energy level. Because the statistics of couplings and fields have no analytic form, one has to use the cavity method widely used in spin glass theory [31]. The cavity method is also known as the belief propagation algorithm, working by iteratively solving a closed equation of cavity quantity, i.e., a spin is virtually removed [29]. The cavity method can thus be used on single instances of ICL. Different weight components are likely strongly correlated, but the cavity marginal  $\eta_{i \rightarrow j}(\sigma_i)$  becomes conditionally independent in the absence of spin  $j$ , which

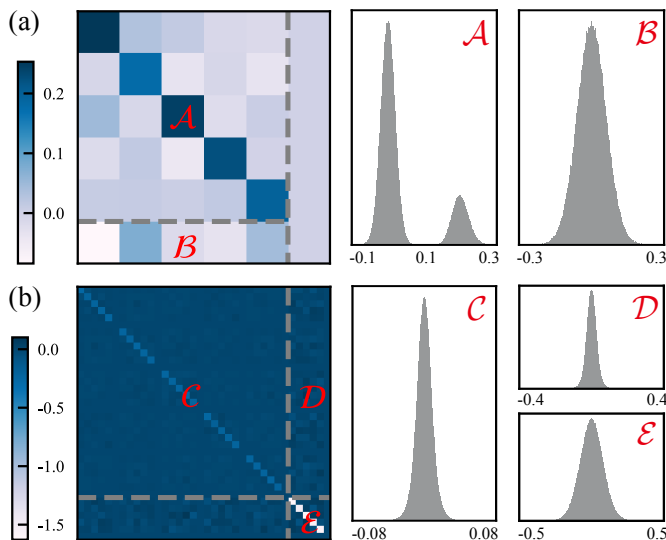


FIG. 1: Statistical properties of the interaction matrix and the external field. (a) The  $\mathbf{H}$  matrix corresponding to the external field  $\mathbf{h}$  has three blocks with different properties:  $\mathcal{A} \in \mathbb{R}^{D \times D}$ ,  $\mathcal{B} \in \mathbb{R}^D$ , and the all-zero vector  $\mathbf{0} \in \mathbb{R}^{D+1}$  (the right-most column). (b) The symmetric  $\mathbf{J}$  matrix also has three different blocks:  $\mathcal{C} \in \mathbb{R}^{D(D+1) \times D(D+1)}$ ,  $\mathcal{D} \in \mathbb{R}^{D(D+1) \times (D+1)}$  and  $\mathcal{E} \in \mathbb{R}^{(D+1) \times (D+1)}$ . The statistics of different blocks are shown in the right panel. For some  $(i, j)$ ,  $J_{ij} = 0$ , but this ratio is  $(2D+1)/(D+1)^2$  since the last column of  $\mathbf{S}$  is an all-zero vector. We count the non-zero values for the distribution. All results are plotted based on an average over 100 000 ensembles of  $(P, D, N) = (1000, 5, 100)$ .

facilitates our derivation of the following self-consistent iteration (namely mean-field equation, see [30] for more details):

$$\eta_{i \rightarrow j}(\sigma_i) = \frac{1}{z_{i \rightarrow j}} e^{\beta h_i \sigma_i - \frac{1}{2} \beta \lambda_i \sigma_i^2} \times \prod_{k \neq i, j} \left[ \int d\sigma_k \eta_{k \rightarrow i}(\sigma_k) e^{\beta J_{ik} \sigma_i \sigma_k} \right], \quad (6)$$

where  $z_{i \rightarrow j}$  is a normalization constant, and  $\eta_{i \rightarrow j}$  is defined as the cavity probability of spin  $\sigma_i$  in the absence of the interaction between spins  $i$  and  $j$ . After the iteration reaches a fixed point, the marginal probability  $\eta_i(\sigma_i)$  of each spin can be calculated by

$$\eta_i(\sigma_i) = \frac{1}{z_i} e^{\beta h_i \sigma_i - \frac{1}{2} \beta \lambda_i \sigma_i^2} \prod_{j \neq i} \int d\sigma_j \eta_{j \rightarrow i}(\sigma_j) e^{\beta J_{ij} \sigma_i \sigma_j}. \quad (7)$$

Because of the continuous nature of spin and weak but dense interactions among spins, we can further simplify the mean-field equation [Eq. (6)], and derive the approximate message passing (AMP) by assuming  $\eta_i(\sigma_i) \sim \mathcal{N}(m_i, v_i)$ , where  $(m_i, v_i)$  is the fixed point of the follow-

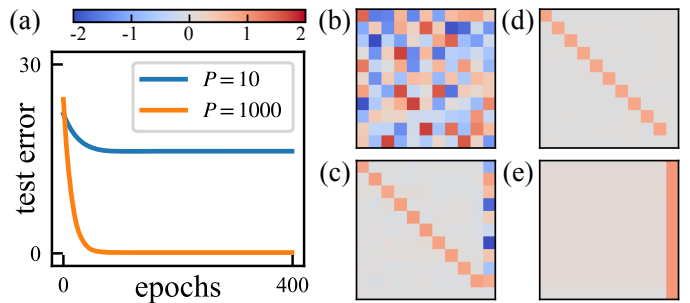


FIG. 2: Test error and the optimal weight matrix of ICL. (a) The test error of the linear attention trained by the stochastic gradient descent (SGD) method for different task diversities. (b) The weight matrix for  $P = 10$  at the end of training. (c) The weight matrix for  $P = 1000$  at the end of training. (d) The weight matrix retrieved from the solution  $\{m_i\}$  of AMP. (e) The variance matrix retrieved from the solution  $\{v_i\}$  of AMP. The color bars are the same with (a).  $(D, N) = (10, 100)$ ,  $\lambda = 0$  for SGD,  $P = 5000$ ,  $(\lambda, \beta) = (0.01, 100)$  for AMP.

ing iterative equation:

$$m_i = \frac{\beta h_i + \beta \sum_{j \neq i} J_{ij} m_j}{\beta \lambda_i - \beta^2 \sum_{j \neq i} J_{ij}^2 v_j}, \quad (8a)$$

$$v_i = \frac{1}{\beta \lambda_i - \beta^2 \sum_{j \neq i} J_{ij}^2 v_j}, \quad (8b)$$

which is also rooted in the Thouless–Anderson–Palmer equation in glass physics [29, 32]. Technical details of deriving the AMP and the self-consistent justification of the Gaussian approximation are given in the appendix (an expanded one is given in [30]).

*Results.*— The iteration of the cavity method depends on the specific form of  $J_{ij}$  and  $h_i$ , which rely on  $S_{m,n}$  defined as  $S_{m,n} = (DN)^{-1} \mathbf{C}_{D+1,m} \mathbf{X}_{n,N+1}$ . The index  $\mu$  is omitted here. The matrix  $\mathbf{S}$  is divided into three blocks: the last column is an all-zero vector [due to the masked label in Eq. (1)], while the other two blocks are labeled as  $\mathcal{A}$  ( $m < D+1, n \neq D+1$ ) and  $\mathcal{B}$  ( $m = D+1, n \neq D+1$ ). As  $h_i = \frac{1}{P} \sum_{\mu} \hat{y}^{\mu} s_i^{\mu}$ , the field matrix has the same block structure with  $\mathbf{S}$  [Fig. 1 (a)]. In addition the interaction matrix  $\mathbf{J}$ , generated by the outer product of the flattened  $\mathbf{S}$  with itself, has three main blocks, labeled as  $\mathcal{C}$ ,  $\mathcal{D}$ , and  $\mathcal{E}$  respectively in Fig. 1 (b).

In contrast to traditional spin glass models [27],  $P(\mathbf{J})$  [or  $P(\mathbf{h})$ ] does not have an analytic form [26], as the coupling or field can be expressed as a complex function of a sum of products of two i.i.d. standard Gaussian random variables (see details in [30]). Therefore, we provide the numerical estimation of the coupling distribution, which all bear a fat tail [Fig. 1 (b)]. We thus define a new type of spin glass model corresponding to ICL, or a metaphor of transformer in large language models.

To see whether our spin glass model captures the correct structure of the weight matrix in the simple trans-

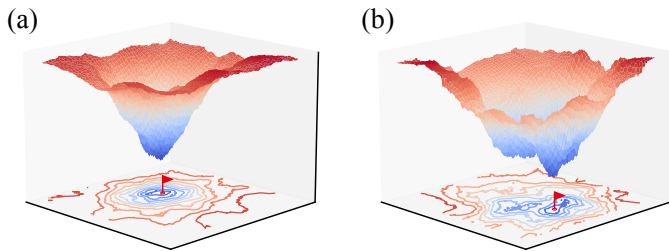


FIG. 3: The energy landscape of the spin glass model for  $P = 1000$  (a) and  $P = 10$  (b). To draw this landscape, we randomly sample 2000 points from the whole weight space when  $D = 10$ ,  $N = 50$ ,  $\lambda = 0.01$ , and calculate their energies by Eq. (12). Then we reduce the weight space with  $(D + 1)^2$  dimension to the two-dimensional plane by t-distributed stochastic neighbor embedding (t-SNE) [33]. The color deep blue indicates lowest energies. The flag on the bottom plane indicates the target weight matrix.

former, we first divide the weight matrix  $\mathbf{W}$  into blocks in the same way as we do for the input matrix, i.e.,

$$\mathbf{W} = \begin{bmatrix} \mathbf{W}_{11} & \mathbf{W}_{12} \\ \mathbf{W}_{21} & \mathbf{W}_{22} \end{bmatrix} \quad (9)$$

where  $\mathbf{W}_{11} \in \mathbb{R}^{D \times D}$ ,  $\mathbf{W}_{12} \in \mathbb{R}^{D \times 1}$ ,  $\mathbf{W}_{21} \in \mathbb{R}^{1 \times D}$ , and  $\mathbf{W}_{22} \in \mathbb{R}$ . In our linear regression task, the actual prediction of the transformer to the test query  $\tilde{\mathbf{x}}$  can be written as

$$\hat{y} = \mathbf{w}^\top (\mathbf{W}_{11} + \mathbf{w}\mathbf{W}_{21}) \tilde{\mathbf{x}}. \quad (10)$$

To derive the above prediction, we have used  $2 \times 2$  block matrix form of  $\mathbf{X}$ , the task  $y = \mathbf{w}^\top \mathbf{x}$ , and the fact of i.i.d.  $\{\mathbf{x}_\ell\}$  (see technical details in [30]). Hence, the weight matrix of a well-trained transformer must satisfy

$$\mathbf{W}_{11} + \mathbf{w}\mathbf{W}_{21} = \mathbf{1}_D. \quad (11)$$

It is clear that, in the case of  $P > 1$ , the weights have a unique optimal solution  $\mathbf{W}_{11} = \mathbf{1}_D$  and  $\mathbf{W}_{21} = 0$ .

In the standard stochastic gradient descent (SGD) training process minimizing Eq. (2), a large value of  $P$  is needed to make the weight matrix converge to the unique solution. In Fig. 2, we show the learning curves and the weight matrix after the training when the amount of training data  $P = 10$  and  $P = 1000$  respectively. By iterating the AMP equations [Eq. (8a) and Eq. (8b)], we get a fixed point of  $\{m_i\}$  and  $\{v_i\}$ , transformed back into the matrix form by inverting  $\Gamma$ . We find that the  $\mathbf{m}$  matrix exhibits the same property as the weight matrix that is well-trained by the SGD. Since the last column of  $\mathbf{W}$  is initialized as  $\mathcal{N}(0, 1)$  and does not participate in the training, the solution of AMP retains the structure of  $m = 0$  and  $v = 1$ . This result shows that our spin glass model captures the properties of practical SGD training [24, 34, 35].

In Fig. 3, we show the energy landscape of our spin glass model. When the task diversity  $P$  is large enough,

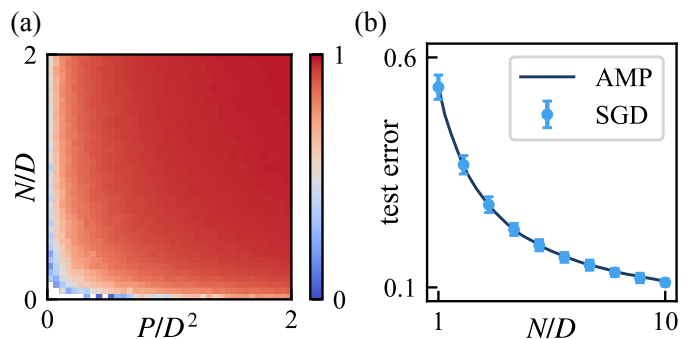


FIG. 4: Results obtained from running the AMP algorithm. (a) The heat map of the contrast  $\mathcal{C}$  with  $D = 40$ ,  $\lambda = 10$ , and  $\beta = 100$ . In the left-bottom corner, AMP does not converge. (b) The test error decreases with the context (prompt) length  $N$ , with  $D = 20$ ,  $\lambda = 0.01$ ,  $P = 10000$ , and  $\beta = 100$ . All the results of AMP and SGD are averaged over 100 trials.

there is only one global minimum in the energy landscape, and the learning can easily reach the lowest energy. When  $P$  is small, there emerge multiple local minima in the energy landscape, and the learning gets easily trapped by metastable states, which prevents the transformer from accurate in-context inference.

To get the phase diagram for single instance pre-training of the transformer, we first define a contrast ratio  $\mathcal{C} = (\langle m_{ii}^2 \rangle - \langle m_{ij}^2 \rangle) / \langle m_{ii}^2 \rangle$ ,  $i \neq j$  to measure whether the model is well trained according to the transformed  $\mathbf{m}$  matrix.  $\mathcal{C} = 1$  means that the model converges to the unique solution, while  $\mathcal{C} = 0$  indicates that the model does not learn the features at all. We show a heat map of the contrast ratio with the rescaled number of the data  $P/D^2$  and the rescaled prompt length  $N/D$  in Fig. 4 (a). The heat map suggests that when the task diversity increases, a smooth transition to perfect generalization occurs, while keeping a large value of task diversity, increasing the prompt length further lowers the generalization error, which is consistent with recent empirical works [19] and theoretical works [21] based on random matrix theory (despite a slightly different setting). In addition, the AMP result coincides perfectly with the SGD [Fig. 4 (b)], which verifies once again that our spin-glass model of ICL is able to predict an unseen embedded function in the test prompts, which is determined by the ground states of  $\mathcal{H}(\sigma)$ . We finally remark that our theory carries over to more complex situations of ICL (see further experiments in [30]).

*Conclusion.*— A fundamental question in large language models is what contributes to the emergence ability of ICL, i.e., why simple next-token prediction-based pre-training leads to in-context learning of previously unseen tasks, especially without further tuning the model parameters. Here, we turn the ICL into a spin glass model and verify the equivalence between the standard SGD training and our statistical mechanic inference. We ob-

serve the fat tail distribution of coupling that determines how the model parameters of the transformer interact with each other. The transformer parameters are akin to an ensemble of real-valued spins in physics whose ground state suggests that the model can infer an unknown function from the shown test prompts after a pre-training of input sequences of sufficient task diversity. The phase diagram for single instance learning is also derived by our method, suggesting a continuous ICL transition.

The spin-glass model mapping of the linear transformer establishes a toy model of understanding emergent abilities such as ICL of large language models. The ground state determines the intelligence boundary, while the task diversity guarantees the accessibility of the ground state. Without a clear understanding of this toy model, it is hard to imagine what are really computed inside the black box of a general transformer in more complex tasks. Future exciting directions include explaining the chain-of-thought prompting [12], i.e., decomposition of a complex task into intermediate steps, and more challenging case of hallucination [36], i.e., the

model could not distinguish the generated outputs from factual knowledge, or it could not understand what they generate [14]. We speculate that this hallucination may be intimately related to the solution space of the spin glass model given a fixed complexity of training dataset, e.g., spurious states in a standard associative memory model, as implied by Eq. (12). These open questions are expected to be addressed in the near future by considering this intriguing physics link, thereby enhancing the robustness and trustworthiness of AI systems.

## ACKNOWLEDGMENTS

This research was supported by the National Natural Science Foundation of China for Grant number 12122515, and Guangdong Provincial Key Laboratory of Magnetolectric Physics and Devices (No. 2022B1212010008), and Guangdong Basic and Applied Basic Research Foundation (Grant No. 2023B1515040023).

## Derivation of cavity method and approximate message passing equation

The spin glass model of the transformer we consider in the main text reads

$$H = - \sum_{i < j} J_{ij} \sigma_i \sigma_j - \sum_i h_i \sigma_i - \frac{\lambda}{2} \sum_i \sigma_i^2, \quad (12)$$

and the Boltzmann distribution of weight configuration can be written as

$$P(\boldsymbol{\sigma}) = \frac{1}{Z} e^{-\beta H(\boldsymbol{\sigma})} = \frac{1}{Z} \prod_i e^{\beta h_i \sigma_i - \frac{\beta \lambda}{2} \sigma_i^2} \prod_{i < j} e^{\beta J_{ij} \sigma_i \sigma_j}, \quad (13)$$

where  $Z$  serves as the partition function. Taking each interaction pair as a factor node and each site term as an external field in Eq. (13), one can write the following cavity iteration in an explicit form according to the standard format of the cavity method (e.g., see the textbook [29]).

$$\eta_{i \rightarrow ij}(\sigma_i) = \frac{1}{z_{i \rightarrow ij}} e^{\beta h_i \sigma_i - \frac{\beta \lambda}{2} \sigma_i^2} \prod_{ik \in \partial i \setminus ij} \eta_{ik \rightarrow i}(\sigma_k), \quad (14)$$

$$\eta_{ij \rightarrow i}(\sigma_i) = \frac{1}{z_{ij \rightarrow i}} \int \prod_{j \in \partial ij \setminus i} d\sigma_j \eta_{j \rightarrow ij}(\sigma_j) e^{\beta J_{ij} \sigma_i \sigma_j}, \quad (15)$$

which is also called the belief propagation equation. The notation  $ij$  denotes an interaction (or factor node in a factor graph representation of the model). Since our model only involves two-body interactions, which means that  $\partial ij \setminus i$  contains only one element  $j$ , the product notation  $\prod_{j \in \partial ij \setminus i}$  can be omitted, and we can simplify the notation  $i \rightarrow ij$  by  $i \rightarrow j$  and  $ij \rightarrow i$  by  $j \rightarrow i$ . Therefore, we can combine Eq. (14) and Eq. (15) together into

$$\eta_{i \rightarrow j}(\sigma_i) = \frac{1}{z_{i \rightarrow j}} e^{\beta h_i \sigma_i - \frac{1}{2} \beta \lambda_i \sigma_i^2} \prod_{k \neq i, j} \left[ \int d\sigma_k \eta_{k \rightarrow i}(\sigma_k) e^{\beta J_{ik} \sigma_i \sigma_k} \right]. \quad (16)$$

After the iteration reaches a fixed point, the marginal probability  $\eta_i(\sigma_i)$  of each spin can be calculated based on the converged cavity marginals as follows

$$\eta_i(\sigma_i) = \frac{1}{z_i} e^{\beta h_i \sigma_i - \frac{1}{2} \beta \lambda_i \sigma_i^2} \prod_{j \neq i} \int d\sigma_j \eta_{j \rightarrow i}(\sigma_j) e^{\beta J_{ij} \sigma_i \sigma_j}. \quad (17)$$

### Relaxed belief propagation

The space complexity to run Eq. (16) is of  $\mathcal{O}(D^4)$ , since  $i = 1, \dots, (D+1)^2$ . To reduce the space complexity, an intuitive approach is to approximate the cavity marginal by a Gaussian distribution  $\mathcal{N}(m_{i \rightarrow j}, v_{i \rightarrow j})$ , and then derive the iterative equations for the first two moments. To validate this intuition, we start from Eq. (16) and apply the Fourier transform and Taylor expansion.

To proceed, we first define  $\xi_{i \rightarrow j} = \sum_{k \neq i, j} \beta J_{ik} \sigma_k$ , and  $G(\xi_{i \rightarrow j}) = e^{\sigma_i \xi_{i \rightarrow j}}$ , and then Eq. (16) can be written as

$$\eta_{i \rightarrow j}(\sigma_i) = \frac{1}{z_{i \rightarrow j}} e^{\beta h_i \sigma_i - \frac{1}{2} \beta \lambda_i \sigma_i^2} \int \prod_{k \neq i, j} [d\sigma_k \eta_{k \rightarrow i}(\sigma_k)] G(\xi_{i \rightarrow j}) \quad (18a)$$

$$= \frac{1}{z_{i \rightarrow j}} e^{\beta h_i \sigma_i - \frac{1}{2} \beta \lambda_i \sigma_i^2} \int \prod_{k \neq i, j} [d\sigma_k \eta_{k \rightarrow i}(\sigma_k)] \int d\hat{\xi}_{i \rightarrow j} \hat{G}(\hat{\xi}_{i \rightarrow j}) e^{i \xi_{i \rightarrow j} \hat{\xi}_{i \rightarrow j}} \quad (18b)$$

$$= \frac{1}{z_{i \rightarrow j}} e^{\beta h_i \sigma_i - \frac{1}{2} \beta \lambda_i \sigma_i^2} \int d\hat{\xi}_{i \rightarrow j} \hat{G}(\hat{\xi}_{i \rightarrow j}) \prod_{k \neq i, j} \int d\sigma_k \eta_{k \rightarrow i}(\sigma_k) \exp \left[ i \hat{\xi}_{i \rightarrow j} (\beta J_{ik} \sigma_k) \right]. \quad (18c)$$

In Eq. (18b), we insert the Fourier transform of  $G(\xi)$ , i.e.,  $\hat{G}(\hat{\xi}_{i \rightarrow j})$ , and absorb irrelevant constants into  $z_{i \rightarrow j}$ . Let us calculate the last integral in Eq. (18c):

$$\mathcal{I} \equiv \int d\sigma_k \eta_{k \rightarrow i}(\sigma_k) \exp \left[ i \hat{\xi} (\beta J_{ik} \sigma_k) \right] \quad (19a)$$

$$= \int d\sigma_k \eta_{k \rightarrow i}(\sigma_k) \left[ 1 + i \hat{\xi} (\beta J_{ik} \sigma_k) - \frac{1}{2} \hat{\xi}^2 (\beta J_{ik} \sigma_k)^2 \right] \quad (19b)$$

$$= 1 + i \hat{\xi} \beta J_{ik} \int d\sigma_k \eta_{k \rightarrow i}(\sigma_k) \sigma_k - \frac{1}{2} \hat{\xi}^2 \beta^2 J_{ik}^2 \int d\sigma_k \eta_{k \rightarrow i}(\sigma_k) \sigma_k^2 \quad (19c)$$

$$= 1 + i \hat{\xi} \beta J_{ik} m_{k \rightarrow i} - \frac{1}{2} \hat{\xi}^2 \beta^2 J_{ik}^2 (v_{k \rightarrow i} + m_{k \rightarrow i}^2) \quad (19d)$$

$$\simeq \exp \left[ i \hat{\xi} \beta J_{ik} m_{k \rightarrow i} - \frac{1}{2} \hat{\xi}^2 \beta^2 J_{ik}^2 v_{k \rightarrow i} \right]. \quad (19e)$$

In Eq. (19b), we use the Taylor expansion of an exponential function, and in Eq. (19c), we define the mean  $m_{k \rightarrow i}$  and the variance  $v_{k \rightarrow i}$  of the message (the cavity marginal probability) as

$$m_{k \rightarrow i} = \int d\sigma_k \eta_{k \rightarrow i}(\sigma_k) \sigma_k, \quad (20)$$

$$v_{k \rightarrow i} = \int d\sigma_k \eta_{k \rightarrow i}(\sigma_k) \sigma_k^2 - m_{k \rightarrow i}^2. \quad (21)$$

In Eq. (19e), we use the fact that the high order power of  $J_{ij}$  are negligible and thus recover the exponential form. Then, we substitute Eq. (19) back to Eq. (18) and obtain

$$\eta_{i \rightarrow j}(\sigma_i) = \frac{1}{z_{i \rightarrow j}} e^{\beta h_i \sigma_i - \frac{1}{2} \beta \lambda_i \sigma_i^2} \int d\hat{\xi}_{i \rightarrow j} \hat{G}(\hat{\xi}_{i \rightarrow j}) \prod_{k \neq i, j} \exp \left[ i \hat{\xi}_{i \rightarrow j} \beta J_{ik} m_{k \rightarrow i} - \frac{1}{2} \hat{\xi}_{i \rightarrow j}^2 \beta^2 J_{ik}^2 v_{k \rightarrow i} \right]. \quad (22)$$

Then, we re-express  $\hat{G}(\hat{\xi}_{i \rightarrow j})$  by  $G(\xi)$  and obtain

$$\eta_{i \rightarrow j}(\sigma_i) = \frac{1}{z_{i \rightarrow j}} e^{\beta h_i \sigma_i - \frac{1}{2} \beta \lambda_i \sigma_i^2} \int d\hat{\xi}_{i \rightarrow j} \int d\xi_{i \rightarrow j} G(\xi_{i \rightarrow j}) e^{-i \xi_{i \rightarrow j} \hat{\xi}_{i \rightarrow j}} \prod_{k \neq i, j} \exp \left[ i \hat{\xi}_{i \rightarrow j} \beta J_{ik} m_{k \rightarrow i} - \frac{1}{2} \hat{\xi}_{i \rightarrow j}^2 \beta^2 J_{ik}^2 v_{k \rightarrow i} \right] \quad (23a)$$

$$= \frac{1}{z_{i \rightarrow j}} e^{\beta h_i \sigma_i - \frac{1}{2} \beta \lambda_i \sigma_i^2} \int d\xi_{i \rightarrow j} G(\xi_{i \rightarrow j}) \times \int d\hat{\xi}_{i \rightarrow j} \exp \left[ -\frac{1}{2} \left( \beta^2 \sum_{k \neq i, j} J_{ik}^2 v_{k \rightarrow i} \right) \hat{\xi}_{i \rightarrow j}^2 + i \left( \beta \sum_{k \neq i, j} J_{ik} m_{k \rightarrow i} - \xi_{i \rightarrow j} \right) \hat{\xi}_{i \rightarrow j} \right] \quad (23b)$$

$$= \frac{1}{z_{i \rightarrow j}} e^{\beta h_i \sigma_i - \frac{1}{2} \beta \lambda_i \sigma_i^2} \int d\xi_{i \rightarrow j} G(\xi_{i \rightarrow j}) \exp \left\{ -\frac{1}{2} \frac{\left( \xi_{i \rightarrow j} - \beta \sum_{k \neq i, j} J_{ik} m_{k \rightarrow i} \right)^2}{\beta^2 \sum_{k \neq i, j} J_{ik}^2 v_{k \rightarrow i}} \right\}. \quad (23c)$$

We can then define the mean and variance of  $\xi_{i \rightarrow j}$  as

$$M_{i \rightarrow j} = \beta \sum_{k \neq i, j} J_{ik} m_{k \rightarrow i}, \quad (24)$$

$$V_{i \rightarrow j} = \beta^2 \sum_{k \neq i, j} J_{ik}^2 v_{k \rightarrow i}. \quad (25)$$

Then, the marginal probability  $\eta_{i \rightarrow j}(\sigma_i)$  can be further calculated as

$$\eta_{i \rightarrow j}(\sigma_i) = \frac{1}{z_{i \rightarrow j}} e^{\beta h_i \sigma_i - \frac{1}{2} \beta \lambda_i \sigma_i^2} \int d\xi_{i \rightarrow j} G(\xi_{i \rightarrow j}) \exp \left[ -\frac{(\xi_{i \rightarrow j} - M_{i \rightarrow j})^2}{2V_{i \rightarrow j}} \right] \quad (26a)$$

$$= \frac{1}{z_{i \rightarrow j}} e^{\beta h_i \sigma_i - \frac{1}{2} \beta \lambda_i \sigma_i^2} \int d\xi_{i \rightarrow j} \exp \left[ -\frac{1}{2} \frac{1}{V_{i \rightarrow j}} \xi_{i \rightarrow j}^2 + \left( \frac{M_{i \rightarrow j}}{V_{i \rightarrow j}} + \sigma_i \right) \xi_{i \rightarrow j} - \frac{M_{i \rightarrow j}^2}{2V_{i \rightarrow j}} \right] \quad (26b)$$

$$= \frac{1}{z_{i \rightarrow j}} e^{\beta h_i \sigma_i - \frac{\beta \lambda_i}{2} \sigma_i^2} \exp \left( M_{i \rightarrow j} \sigma_i + \frac{1}{2} V_{i \rightarrow j} \sigma_i^2 \right) \quad (26c)$$

$$= \frac{1}{z_{i \rightarrow j}} \exp \left[ -\frac{1}{2} (\beta \lambda_i - V_{i \rightarrow j}) \sigma_i^2 + (\beta h_i + M_{i \rightarrow j}) \sigma_i \right]. \quad (26d)$$

Equation (26d) implies that  $\eta_{i \rightarrow j}(\sigma_i)$  follows a Gaussian distribution with the following mean and variance

$$m_{i \rightarrow j} = \frac{\beta h_i + M_{i \rightarrow j}}{\beta \lambda_i - V_{i \rightarrow j}}, \quad (27)$$

$$v_{i \rightarrow j} = \frac{1}{\beta \lambda_i - V_{i \rightarrow j}}. \quad (28)$$

Now, we have obtained the so-called relaxed belief propagation (r-BP) equation:

$$\begin{cases} M_{i \rightarrow j} = \beta \sum_{k \neq i, j} J_{ik} m_{k \rightarrow i}, \\ V_{i \rightarrow j} = \beta^2 \sum_{k \neq i, j} J_{ik}^2 v_{k \rightarrow i}, \end{cases} \quad \begin{cases} m_{i \rightarrow j} = \frac{\beta h_i + M_{i \rightarrow j}}{\beta \lambda_i - V_{i \rightarrow j}}, \\ v_{i \rightarrow j} = \frac{1}{\beta \lambda_i - V_{i \rightarrow j}}. \end{cases} \quad (29)$$

Compared to the original belief propagation equation, the r-BP equations do not require a numerical integration, thereby improving the computational efficiency. Moreover, it provides a basis for deriving the AMP equation shown in the main text. After the relaxed belief propagation equation converges, we get further the marginal probability as

$$\eta_i(\sigma_i) = \frac{1}{z_i} e^{\beta h_i \sigma_i - \frac{1}{2} \beta \lambda_i \sigma_i^2} \prod_{j \neq i} \left\{ \int d\sigma_j \exp \left[ -\frac{1}{2} (\beta \lambda_j - V_{j \rightarrow i}) \sigma_j^2 + (\beta h_j + \beta J_{ij} \sigma_i + M_{j \rightarrow i}) \sigma_j \right] \right\} \quad (30a)$$

$$= \frac{1}{z_i} e^{\beta h_i \sigma_i - \frac{1}{2} \beta \lambda_i \sigma_i^2} \prod_{j \neq i} \exp \left[ \frac{(\beta h_j + \beta J_{ij} \sigma_i + M_{j \rightarrow i})^2}{2(\beta \lambda_j - V_{j \rightarrow i})} \right] \quad (30b)$$

$$= \frac{1}{z_i} \exp \left[ -\frac{1}{2} \left( \beta \lambda_i - \sum_{j \neq i} \beta^2 J_{ij}^2 v_{j \rightarrow i} \right) \sigma_i^2 + \left( \beta h_i + \sum_{j \neq i} \beta J_{ij} m_{j \rightarrow i} \right) \sigma_i \right]. \quad (30c)$$

As we expected, Eq. (30c) suggests that  $\eta_i(\sigma_i)$  indeed follows a Gaussian distribution  $\mathcal{N}(m_i, v_i)$ , with the following mean and variance

$$m_i = \frac{\beta h_i + \beta \sum_{j \neq i} J_{ij} m_{j \rightarrow i}}{\beta \lambda_i - \beta^2 \sum_{j \neq i} J_{ij}^2 v_{j \rightarrow i}}, \quad v_i = \frac{1}{\beta \lambda_i - \beta^2 \sum_{j \neq i} J_{ij}^2 v_{j \rightarrow i}}, \quad (31)$$

where  $m_{j \rightarrow i}$  and  $v_{j \rightarrow i}$  are the fixed points of the r-BP iterative equations [Eq. (29)]. To conclude, the intuition of Gaussian approximation is theoretically justified.

### Approximate message passing equation

If we can remove the directed arrows (e.g.,  $i \rightarrow j$ ) in the r-BP, the space complexity of the algorithm can be greatly reduced, reducing from  $\mathcal{O}(D^4)$  to  $\mathcal{O}(D^2)$ . We next show how this can be possible. By using the following identities  $M_i = M_{i \rightarrow j} + \beta J_{ij} m_{j \rightarrow i}$  and  $V_i = V_{i \rightarrow j} + \beta^2 J_{ij}^2 v_{j \rightarrow i}$ , we further find that

$$m_i - m_{i \rightarrow j} = \frac{\beta h_i + M_i}{\beta \lambda - V_i} - \frac{\beta h_i + M_{i \rightarrow j}}{\beta \lambda - V_{i \rightarrow j}} = \frac{\beta J_{ij} m_{j \rightarrow i} (\beta \lambda_i - V_i) + \beta^2 J_{ij}^2 v_{j \rightarrow i} (\beta h_i + M_i)}{\beta^2 \lambda_i^2 - 2\beta \lambda_i V_i + V_i^2} \sim \mathcal{O}\left(\frac{1}{D^2}\right), \quad (32)$$

and

$$v_i - v_{i \rightarrow j} = \frac{1}{\beta \lambda - V_i} - \frac{1}{\beta \lambda - V_{i \rightarrow j}} = \frac{\beta^2 J_{ij}^2 v_{j \rightarrow i}}{\beta^2 \lambda_i^2 - 2\beta \lambda_i V_i + V_i^2} \sim \mathcal{O}\left(\frac{1}{D^4}\right). \quad (33)$$

In the large  $D$  limit (or even only  $D$  is not too small), we can further simplify the relaxed belief propagation equation to the AMP equation

$$m_i = \frac{\beta h_i + \beta \sum_{j \neq i} J_{ij} m_j}{\beta \lambda_i - \beta^2 \sum_{j \neq i} J_{ij}^2 v_j}, \quad (34a)$$

$$v_i = \frac{1}{\beta \lambda_i - \beta^2 \sum_{j \neq i} J_{ij}^2 v_j}. \quad (34b)$$

In this case, we only need to iterate the above two equations of  $(m_i, v_i)$  to obtain the fixed points. This AMP equation saves  $(D+1)^2$ -fold space complexity for running the algorithm if we record  $(D+1)^2$  as the number of spins in the system. In different forms, the AMP equation was first discovered in a statistical mechanics analysis of signal transmission problem [37], and is also rooted in the Thouless–Anderson–Palmer equation in glass physics [29, 31, 32].

### Derivation of the unique optimal solution to the linear attention transformer

In this section, we provide a detailed derivation of the unique optimal solution to the linear attention transformer [i.e., Eq. (10) and Eq. (11) in the main text]. The input matrix  $\mathbf{X}$  and the weight matrix  $\mathbf{W}$  can be represented as  $2 \times 2$  block matrices

$$\mathbf{X} = \begin{bmatrix} \mathbf{X}_0 & \tilde{\mathbf{x}} \\ \mathbf{y}_0^\top & 0 \end{bmatrix}, \quad \mathbf{W} = \begin{bmatrix} \mathbf{W}_{11} & \mathbf{W}_{12} \\ \mathbf{W}_{21} & \mathbf{W}_{22} \end{bmatrix}, \quad (35)$$

where  $\mathbf{X}_0 = \{\mathbf{x}_1, \mathbf{x}_2, \dots, \mathbf{x}_N\} \in \mathbb{R}^{D \times N}$  denotes the data used for the prompts,  $\mathbf{y}_0 = \mathbf{X}_0^\top \mathbf{w}$  is the corresponding label vector, and  $\tilde{\mathbf{x}}$  is the testing prompt whose label needs to be predicted by the transformer. The blocks of the weight matrix  $\mathbf{W}$  have the same size as the corresponding blocks of  $\mathbf{X}$ , with  $\mathbf{W}_{11} \in \mathbb{R}^{D \times D}$ ,  $\mathbf{W}_{12} \in \mathbb{R}^{D \times 1}$ ,  $\mathbf{W}_{21} \in \mathbb{R}^{1 \times D}$ , and  $\mathbf{W}_{22} \in \mathbb{R}$ . Thus, we can calculate

$$\mathbf{X}\mathbf{X}^\top = \begin{bmatrix} \mathbf{X}_0 & \tilde{\mathbf{x}} \\ \mathbf{y}_0^\top & 0 \end{bmatrix} \begin{bmatrix} \mathbf{X}_0^\top & \mathbf{y}_0 \\ \tilde{\mathbf{x}}^\top & 0 \end{bmatrix} = \begin{bmatrix} \mathbf{X}_0 \mathbf{X}_0^\top + \tilde{\mathbf{x}} \tilde{\mathbf{x}}^\top & \mathbf{X}_0 \mathbf{y}_0 \\ \mathbf{y}_0^\top \mathbf{X}_0^\top & \mathbf{y}_0^\top \mathbf{y}_0 \end{bmatrix}, \quad (36)$$

and

$$\mathbf{W}\mathbf{X} = \begin{bmatrix} \mathbf{W}_{11} & \mathbf{W}_{12} \\ \mathbf{W}_{21} & \mathbf{W}_{22} \end{bmatrix} \begin{bmatrix} \mathbf{X}_0 & \tilde{\mathbf{x}} \\ \mathbf{y}_0^\top & 0 \end{bmatrix} = \begin{bmatrix} \mathbf{W}_{11} \mathbf{X}_0 + \mathbf{W}_{12} \mathbf{y}_0^\top & \mathbf{W}_{11} \tilde{\mathbf{x}} \\ \mathbf{W}_{21} \mathbf{X}_0 + \mathbf{W}_{22} \mathbf{y}_0^\top & \mathbf{W}_{21} \tilde{\mathbf{x}} \end{bmatrix}. \quad (37)$$

Considering the prediction of the transformer  $\hat{y} = \mathbf{Y}_{D+1, N+1} = \frac{1}{DN} (\mathbf{X}\mathbf{X}^\top \mathbf{W}\mathbf{X})_{D+1, N+1}$ , using  $2 \times 2$  block matrix multiplication, one obtains the following result:

$$\hat{y} = \gamma \mathbf{y}_0^\top \mathbf{X}_0^\top \mathbf{W}_{11} \tilde{\mathbf{x}} + \gamma \mathbf{y}_0^\top \mathbf{y}_0 \mathbf{W}_{21} \tilde{\mathbf{x}} \quad (38a)$$

$$= \gamma (\mathbf{X}_0^\top \mathbf{w})^\top \mathbf{X}_0^\top \mathbf{W}_{11} \tilde{\mathbf{x}} + \gamma (\mathbf{X}_0^\top \mathbf{w})^\top (\mathbf{X}_0^\top \mathbf{w}) \mathbf{W}_{21} \tilde{\mathbf{x}} \quad (38b)$$

$$= \gamma \mathbf{w}^\top \mathbf{X}_0 \mathbf{X}_0^\top \mathbf{W}_{11} \tilde{\mathbf{x}} + \gamma \mathbf{w}^\top \mathbf{X}_0 \mathbf{X}_0^\top \mathbf{w} \mathbf{W}_{21} \tilde{\mathbf{x}} \quad (38c)$$

$$= \mathbf{w}^\top (\mathbf{W}_{11} + \mathbf{w} \mathbf{W}_{21}) \tilde{\mathbf{x}}, \quad (38d)$$



where  $\gamma = (DN)^{-1}$ , the definition  $\mathbf{y}_0 = \mathbf{X}_0^\top \mathbf{w}$  is used to obtain Eq. (38b), and the approximation  $\frac{1}{N} \mathbf{X}_0 \mathbf{X}_0^\top = \mathbf{I}$  for the large  $N$  is used to obtain Eq. (38d). Note that the prefactor  $\gamma$  in the actual output is implied in the above derivation to keep the output being of the order unity. Comparing the actual prediction with the true label  $\tilde{\mathbf{y}} = \mathbf{w}^\top \tilde{\mathbf{x}}$  corresponding to  $\tilde{\mathbf{x}}$ , one finds that the optimal solution for the weight matrix must satisfy the following condition:

$$\mathbf{W}_{11}^* + \mathbf{w} \mathbf{W}_{21}^* = \mathbf{1}_D. \quad (39)$$

Equation (39) is actually a set of linear equations, which can be written in the form of  $\mathbf{A} \mathbf{x} = \mathbf{b}$  where  $\{x_i\}$  indicates the weight components to be determined. The number of variables in the equations is  $D^2 + D$ . Given an input matrix  $\mathbf{X}$  generated by a specific  $\mathbf{w}$ , we can write down  $D^2$  equations to solve for the optimal weight. Therefore, the mathematics of linear equations tells us that when the number of input matrices  $P = 1$ , the weight matrix  $\mathbf{W}$  has infinitely many solutions. However, as long as  $P > 1$ , the set of equations has a unique solution, which can be readily deduced as  $\mathbf{W}_{11}^* = \mathbf{1}_D$  and  $\mathbf{W}_{21}^* = \mathbf{0}$ . In practice, the transformer or our spin glass model needs a larger value of  $P$  to identify this optimal matrix.

### Statistics of elements in different blocks of the $\mathbf{S}$ matrix and the Interaction matrix $\mathbf{J}$

The block structure of the  $\mathbf{S}$  matrix looks the same with that of field matrix  $\mathbf{H}$  in Fig. 1 (a) of the main text. By definition, the matrix  $\mathbf{S}$  is divided into three blocks: the last column is an all-zero vector (due to the masked label in the input matrix), while the other two blocks are labeled as  $\mathcal{A}$  ( $m < D + 1, n \neq D + 1$ ) and  $\mathcal{B}$  ( $m = D + 1, n \neq D + 1$ ). We present here the explicit formulation of the elements in each block. We denote the distribution of elements in the block  $\mathcal{A}$  as  $P(\mathcal{A})$ , and similar notations for other blocks.

- $P(\mathcal{A})$  is equivalent to  $P(z)$ , where  $z = u \sum_i v_i \sum_j w_j x_{ij}$ ;
- $P(\mathcal{B})$  is equivalent to  $P(\theta)$ , where  $\theta = u \sum_i (\sum_j w_j x_{ij})^2$ ;
- $P(\mathcal{C})$  is equivalent to  $P(\xi_1)$ , where  $\xi_1 = z_1 z_2$ , and  $z_1, z_2 \sim P(z)$ ;
- $P(\mathcal{D})$  is equivalent to  $P(\xi_2)$ , where  $\xi_2 = z \theta$ , and  $z \sim P(z)$ ,  $\theta \sim P(\theta)$ ;
- $P(\mathcal{E})$  is equivalent to  $P(\xi_3)$ , where  $\xi_3 = \theta_1 \theta_2$ , and  $\theta_1, \theta_2 \sim P(\theta)$ .

All the variables  $u, v, w, x$  used above are i.i.d. standard Gaussian random variables.

A surprising observation is that the distributions of blocks  $\mathcal{A}$ ,  $\mathcal{B}$  and  $\mathcal{E}$  before and after increasing the prompt length are almost the same, while the blocks  $\mathcal{C}$  and  $\mathcal{D}$  seem sensitive to the change of the prompt length (see Fig. 5, but a weaker effect for  $\mathcal{D}$ ). However, once  $P$  is sufficiently large, the correct weight solution will be learned, and thus the transformer achieves a nearly perfect in-context inference, which captures the essence of ICL explained in the main text.

### Generalization to more complex attention structures

In this section, we verify whether our spin glass model is robust to more complex attention structures in transformers, by carrying out extensive experimental simulations. The linear attention setting used in the main text is called simplified linear attention (SLA) in this section. The explicit formulation is given below.

$$\mathbf{Y}_{\text{SLA}} = \frac{1}{DN} \mathbf{X} \mathbf{X}^\top \mathbf{W} \mathbf{X}, \quad (40)$$

where  $\mathbf{W} \equiv \mathbf{W}_Q^\top \mathbf{W}_K$ . This SLA will be compared with the case of removing the softmax function yet keeping the value matrix trainable, which we call the full linear attention (FLA) as follows.

$$\mathbf{Y}_{\text{FLA}} = \frac{1}{DN\sqrt{D}} \mathbf{W}_V \mathbf{X} \mathbf{X}^\top \mathbf{W} \mathbf{X}. \quad (41)$$

The single-head full softmax attention (SA) defined below is also compared.

$$\mathbf{Y}_{\text{SA}} = \mathbf{W}_V \mathbf{X} \cdot \text{Softmax} \left( \frac{(\mathbf{W}_Q \mathbf{X})^\top \mathbf{W}_K \mathbf{X}}{\sqrt{D}} \right). \quad (42)$$

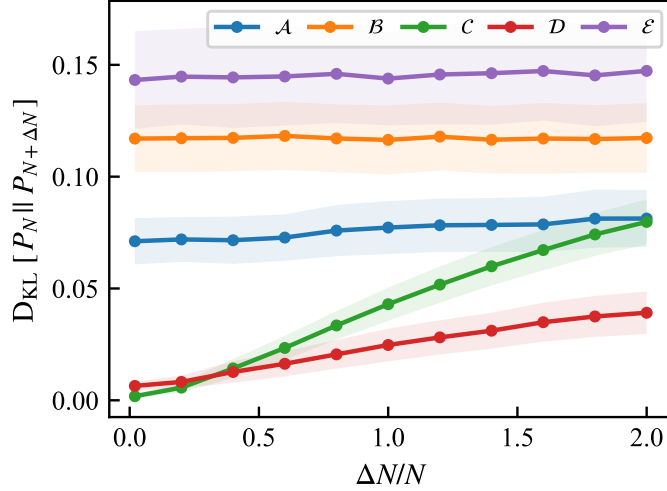


FIG. 5: The KL divergence  $D_{\text{KL}}[P_N \| P_{N+\Delta N}]$  between the original distribution of the elements in blocks shown in Fig.1 of the main text and that with the prompt length  $N$  prolonged by  $\Delta N$ .  $(P, D, N) = (1000, 20, 50)$ . The results are averaged over 1000 examples.

It is important to note that defining  $\mathbf{W} \equiv \mathbf{W}_Q^\top \mathbf{W}_K$  in the linear attention case is not a simplification.

A full transformer network consists of an embedding layer, encoder blocks, and decoder blocks [5]. For our linear regression task, we do not need an embedding layer. An encoder block includes two parts. The first part is the self-attention mechanism, aiming to evaluate the correlations among tokens in the input block  $\mathbf{X}$ . To this end, we introduce three trainable matrices, namely, query ( $Q$ ), key ( $K$ ), and value ( $V$ ). Then, a linear transformation of the input is applied as follows.

$$\begin{aligned} \mathbf{Q} &= \mathbf{W}_Q \cdot \mathbf{X}, \\ \mathbf{K} &= \mathbf{W}_K \cdot \mathbf{X}, \\ \mathbf{V} &= \mathbf{W}_V \cdot \mathbf{X}, \end{aligned} \quad (43)$$

where  $\mathbf{W}_Q, \mathbf{W}_K \in \mathbb{R}^{H \times (D+1)}$  and  $\mathbf{W}_V \in \mathbb{R}^{H \times (D+1)}$  are  $Q, K, V$  matrices respectively, and  $H$  is the internal size of the attention operation. Therefore, we define  $X_t$  as the  $t$ -th column of  $\mathbf{X}$ , and then we can define three vectors, namely  $\mathbf{k}_t = \mathbf{W}_K X_t$ ,  $\mathbf{v}_t = \mathbf{W}_V X_t$ , and  $\mathbf{q}_t = \mathbf{W}_Q X_t$ . Then, the  $t$ -th column of the self-attention matrix  $\text{SA}(\mathbf{X})$  is given by

$$\begin{aligned} \text{attn}(t) &= \sum_{i=1}^{N+1} \alpha_i(t) \mathbf{v}_i, \\ \alpha_i(t) &= \frac{e^{\mathbf{k}_i^\top \mathbf{q}_t / \sqrt{H}}}{\sum_{j=1}^{N+1} e^{\mathbf{k}_j^\top \mathbf{q}_t / \sqrt{H}}}, \end{aligned} \quad (44)$$

where  $\alpha_i(t)$  is a softmax operation containing information about the pairwise interactions between tokens. The normalization factor  $\sqrt{H}$  is required to retain relevant quantities in the exponential function being of the order one. The second part is two feed-forward layers with skip connection, i.e.,

$$\begin{aligned} \mathbf{z}_1 &= \text{SA}(\mathbf{X}) + \mathbf{X} && \text{(residual layer 1)} \\ \mathbf{z}_2 &= \text{ReLU}(W_1 \cdot \mathbf{z}_1 + b_1) && \text{(feed-forward layer 1)} \\ \mathbf{z}_3 &= W_2 \cdot \mathbf{z}_2 + b_2 && \text{(feed-forward layer 2)} \\ \mathbf{z}^{\text{out}} &= \mathbf{z}_1 + \mathbf{z}_3 && \text{(residual layer 2)} \end{aligned} \quad (45)$$

where  $W_1, W_2$  and  $b_1, b_2$  are weights and biases of the two feed-forward layers. We call this complex layered transformer structure as TF.

In addition, the transformer usually employs the multi-head attention structure. Therefore, for comparison, we further consider a multi-head linear attention model (MHLA), where the multiple outputs of Eq. (41) (one output

corresponds to one head) are concatenated and then linearly read through a learnable readout matrix  $\mathbf{W}_O$ . We denote the number of attention heads, i.e., the dimension of the linear readout, as  $M$ .

We leave exploration of more complex tasks beyond linear regression and more complex transformers such as repeated transformer blocks together with multi-headed structures to future works. The current experiments are sufficient to justify our theory of spin-glass mapping. The experimental results of the above different models are shown in Fig. 6. Figure 6 shows the robustness of our theory against different transformer settings, although SA and TF display a higher test error. This can be understood as the linear attention structure is more computable for the linear regression task compared to the non-linear softmax attention. For the softmax attention and more advanced structures, it is hard to derive such concise results as in Sec , and an Ising spin glass model specified in the main text. However, the ground state interpretation of the learning is not a specific picture, and the underlying mechanism for the ICL in the simple but non-trivial setting we consider can be analytically clarified, thereby offering a promising avenue for thinking about how to model many intriguing but puzzling properties of large language models.

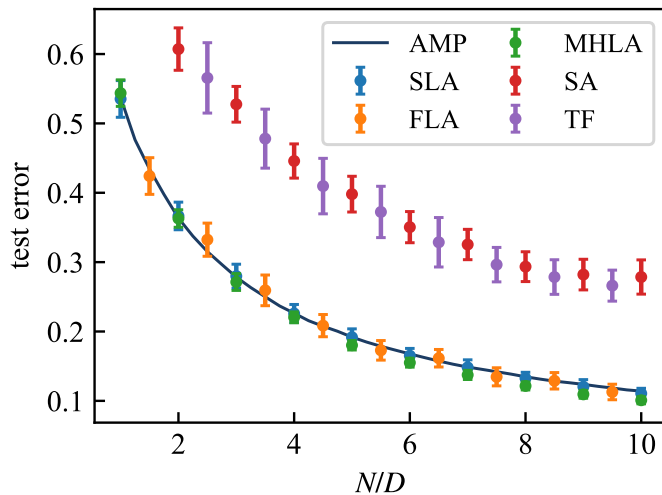


FIG. 6: Comparison of generalization errors for different transformer settings.  $\lambda = 0.01$ ,  $P = 10\,000$ ,  $D = 20$ , and  $\beta = 100$  for AMP. For SA and TF,  $H = 32$ .  $M = 10$  for MHLA. Results are averaged over 100 independent trials.

---

\* Electronic address: huanghp7@mail.sysu.edu.cn

- [1] Yoshua Bengio, Réjean Ducharme, Pascal Vincent, and Christian Janvin. A neural probabilistic language model. *J. Mach. Learn. Res.*, 3:1137–1155, 2003.
- [2] Tomas Mikolov, Ilya Sutskever, Kai Chen, Greg Corrado, and Jeffrey Dean. Distributed representations of words and phrases and their compositionality. In *Proceedings of the 26th International Conference on Neural Information Processing Systems - Volume 2*, NIPS’13, pages 3111–3119, Red Hook, NY, USA, 2013. Curran Associates Inc.
- [3] Kyunghyun Cho, Bart van Merriënboer, Caglar Gulcehre, Dzmitry Bahdanau, Fethi Bougares, Holger Schwenk, and Yoshua Bengio. Learning phrase representations using rnn encoder-decoder for statistical machine translation. In *Proceedings of the 2014 Conference on Empirical Methods in Natural Language Processing (EMNLP)*, pages 1724–1734. Association for Computational Linguistics, 2014.
- [4] Dzmitry Bahdanau, Kyunghyun Cho, and Yoshua Bengio. Neural machine translation by jointly learning to align and translate. In *ICLR 2015 : International Conference on Learning Representations 2015*, 2015.
- [5] Ashish Vaswani, Noam Shazeer, Niki Parmar, Jakob Uszkoreit, Llion Jones, Aidan N. Gomez, Lukasz Kaiser, and Illia Polosukhin. Attention is all you need. In *Proceedings of the 31st International Conference on Neural Information Processing Systems*, NIPS’17, pages 6000–6010, Red Hook, NY, USA, 2017. Curran Associates Inc.
- [6] Eran Malach. Auto-regressive next-token predictors are universal learners. *arXiv:2309.06979*, 2023.
- [7] Chan Li, Junbin Qiu, and Haiping Huang. Meta predictive learning model of languages in neural circuits. *Phys. Rev. E*, 109:044309, 2024.
- [8] Sébastien Bubeck, Varun Chandrasekaran, Ronen Eldan, John A. Gehrke, Eric Horvitz, Ece Kamar, Peter Lee, Yin Tat Lee, Yuan-Fang Li, Scott M. Lundberg, Harsha Nori, Hamid Palangi, Marco Tulio Ribeiro, and Yi Zhang. Sparks of artificial general intelligence: Early experiments with gpt-4. *arXiv:2303.12712*, 2023.
- [9] Tom Brown, Benjamin Mann, Nick Ryder, Melanie Subbiah, Jared D Kaplan, Prafulla Dhariwal, Arvind Neelakantan,

- Pranav Shyam, Girish Sastry, Amanda Askell, Sandhini Agarwal, Ariel Herbert-Voss, Gretchen Krueger, Tom Henighan, Rewon Child, Aditya Ramesh, Daniel Ziegler, Jeffrey Wu, Clemens Winter, Chris Hesse, Mark Chen, Eric Sigler, Mateusz Litwin, Scott Gray, Benjamin Chess, Jack Clark, Christopher Berner, Sam McCandlish, Alec Radford, Ilya Sutskever, and Dario Amodei. Language models are few-shot learners. In H. Larochelle, M. Ranzato, R. Hadsell, M.F. Balcan, and H. Lin, editors, *Advances in Neural Information Processing Systems*, volume 33, pages 1877–1901. Curran Associates, Inc., 2020.
- [10] Alec Radford, Jeff Wu, Rewon Child, David Luan, Dario Amodei, and Ilya Sutskever. Language models are unsupervised multitask learners. *OpenAI blog*, 1:9, 2019.
- [11] Jared Kaplan, Sam McCandlish, Tom Henighan, Tom B Brown, Benjamin Chess, Rewon Child, Scott Gray, Alec Radford, Jeffrey Wu, and Dario Amodei. Scaling laws for neural language models. *arXiv:2001.08361*, 2020.
- [12] Jason Wei, Yi Tay, Rishi Bommasani, Colin Raffel, Barret Zoph, Sebastian Borgeaud, Dani Yogatama, Maarten Bosma, Denny Zhou, Donald Metzler, Ed H. Chi, Tatsunori Hashimoto, Oriol Vinyals, Percy Liang, Jeff Dean, and William Fedus. Emergent abilities of large language models. *Transactions on Machine Learning Research*, 2022.
- [13] Micah Goldblum, Anima Anandkumar, Richard Baraniuk, Tom Goldstein, Kyunghyun Cho, Zachary C Lipton, Melanie Mitchell, Preetum Nakkiran, Max Welling, and Andrew Gordon Wilson. Perspectives on the state and future of deep learning - 2023. *arXiv:2312.09323*, 2023.
- [14] Haiping Huang. Eight challenges in developing theory of intelligence. *Front. Comput. Neurosci.*, 18:1388166, 2024.
- [15] Johannes Von Oswald, Eyvind Niklasson, Ettore Randazzo, João Sacramento, Alexander Mordvintsev, Andrey Zhmoginov, and Max Vladymyrov. Transformers learn in-context by gradient descent. In *International Conference on Machine Learning*, pages 35151–35174, 2023.
- [16] Alberto Bietti, Vivien Cabannes, Diane Bouchacourt, Herve Jegou, and Leon Bottou. Birth of a transformer: A memory viewpoint. *arXiv:2306.00802*, 2023.
- [17] Shivam Garg, Dimitris Tsipras, Percy S Liang, and Gregory Valiant. What can transformers learn in-context? a case study of simple function classes. *Advances in Neural Information Processing Systems*, 35:30583–30598, 2022.
- [18] Sang Michael Xie, Aditi Raghunathan, Percy Liang, and Tengyu Ma. An explanation of in-context learning as implicit bayesian inference. *arXiv:2111.02080*, 2021.
- [19] Allan Raventós, Mansheej Paul, Feng Chen, and Surya Ganguli. Pretraining task diversity and the emergence of non-bayesian in-context learning for regression. In A. Oh, T. Naumann, A. Globerson, K. Saenko, M. Hardt, and S. Levine, editors, *Advances in Neural Information Processing Systems*, volume 36, pages 14228–14246. Curran Associates, Inc., 2023.
- [20] Yingcong Li, Muhammed Emrullah Ildiz, Dimitris Papailiopoulos, and Samet Oymak. Transformers as algorithms: Generalization and stability in in-context learning. In *International Conference on Machine Learning*, pages 19565–19594, 2023.
- [21] Yue M. Lu, Mary I. Letey, Jacob A. Zavatone-Veth, Anindita Maiti, and Cengiz Pehlevan. Asymptotic theory of in-context learning by linear attention. *arXiv:2405.11751*, 2024.
- [22] Jingfeng Wu, Difan Zou, Zixiang Chen, Vladimir Braverman, Quanquan Gu, and Peter L. Bartlett. How many pretraining tasks are needed for in-context learning of linear regression? *arXiv:2310.08391*, 2024. in ICLR 2024.
- [23] Ekin Akyürek, Dale Schuurmans, Jacob Andreas, Tengyu Ma, and Denny Zhou. What learning algorithm is in-context learning? investigations with linear models. *arXiv:2211.15661*, 2022.
- [24] Ruiqi Zhang, Spencer Frei, and Peter L. Bartlett. Trained transformers learn linear models in-context. *Journal of Machine Learning Research*, 25(49):1–55, 2024.
- [25] Kwangjun Ahn, Xiang Cheng, Minhak Song, Chulhee Yun, Ali Jadbabaie, and Suvrit Sra. Linear attention is (maybe) all you need (to understand transformer optimization). *arXiv:2310.01082*, in ICLR, 2024.
- [26] M. D. Springer and W. E. Thompson. The distribution of products of beta, gamma and gaussian random variables. *SIAM Journal on Applied Mathematics*, 18(4):721–737, 1970.
- [27] A. Crisanti and H. J. Sommers. The spherical p-spin interaction spin glass model: the statics. *Zeitschrift für Physik B Condensed Matter*, 87(3):341–354, 1992.
- [28] Giacomo Gradenigo, Maria Chiara Angelini, Luca Leuzzi, and Federico Ricci-Tersenghi. Solving the spherical p-spin model with the cavity method: equivalence with the replica results. *Journal of Statistical Mechanics: Theory and Experiment*, 2020(11):113302, 2020.
- [29] Haiping Huang. *Statistical Mechanics of Neural Networks*. Springer, Singapore, 2022.
- [30] See the supplemental material at <http://...> for technical and experimental details, which includes Ref. [21, 29, 31, 32, 37].
- [31] M. Mézard, G. Parisi, and M. A. Virasoro. *Spin Glass Theory and Beyond*. World Scientific, Singapore, 1987.
- [32] P. W. Anderson D. J. Thouless and R. G. Palmer. Solution of 'solvable model of a spin glass'. *Phil. Mag.*, 35(3):593–601, 1977.
- [33] Laurens van der Maaten and Geoffrey Hinton. Visualizing data using t-sne. *Journal of Machine Learning Research*, 9(86):2579–2605, 2008.
- [34] Siyu Chen, Heejune Sheen, Tianhao Wang, and Zhuoran Yang. Training dynamics of multi-head softmax attention for in-context learning: Emergence, convergence, and optimality. *arXiv:2402.19442*, 2024.
- [35] Yu Huang, Yuan Cheng, and Yingbin Liang. In-context convergence of transformers. *arXiv:2310.05249*, 2023.
- [36] Sebastian Farquhar, Jannik Kossen, Lorenz Kuhn, and Yarin Gal. Detecting hallucinations in large language models using semantic entropy. *Nature*, 630(8017):625–630, 2024.
- [37] Yoshiyuki Kabashima. A cdma multiuser detection algorithm on the basis of belief propagation. *Journal of Physics A: Mathematical and General*, 36(43):11111, 2003.